MAUSAM, **66**, 2 (April 2015), 299-310

550.34 (540.27)

Detection of fractured zones in part of hard rock area of Mirzapur District, Uttar Pradesh, using integrated geophysical method

RAJAN KUMAR and G. S. YADAV

Department of Geophysics, Banaras Hindu University, Varanasi, India

(*Received 29 August 2013, Modified 18 February 2014*)

e mail : rajan.08.ism@gmail.com

सार - भारत के उत्तर प्रदेश के मिर्जापुर जिले में सख्त चट्टानी क्षेत्र वाले हिस्से में दरार वाले क्षेत्र के स्थान का निर्धारण करने के लिए, अत्यधिक न्यून आवृत्ति वाले वैद्युत चुम्बकत्व (VLF-EM) के वास्तविक घटक के विश्लेषणात्मक सिग्नल के विस्तार और प्रतिरोधात्मक पद्धति का उपयोग किया गया है। समाकलित भू-भैतिकी सर्वेक्षणों का उपयोग करते हुए उपयुक्त स्थानों के लिए पूर्व सूचनाओं के अतिरिक्त रेखाओं की रूपरेखा प्रस्तुत करने के लिए उपग्रह बिम्बावली का उपयोग किया गया। छः VLF टेढ़े-मेढ़े पथों के प्रोफाइलों के साथ VLF-EM आँकड़ा प्राप्त किया गया। VLF-EM आँकड़ा के वास्तविक घटक के विश्लेषणात्मक सिग्नल के हिलबर्ट ट्रांसफार्म और विस्तार के साथ जोड़ने वाले फ्रासर और करावस- जेल्ट फिल्टरों तथा प्रोफाइल चित्र के रूप में वास्तविक घटक के 2-D विश्लेषणात्मक सिग्नल के विस्तार का उपयोग करते हुए परिणाम प्राप्त किए गए। हिल्बर्ट ट्रांसफार्म के वास्तविक घटक, सख्त चट्टानी क्षेत्र के हिस्से में दरार वाले क्षेत्र में अधिकतम गहराई की उत्पत्ति करते हैं। इन्हें प्रतिरोधकता परिज्ञापन और भू वैद्युत क्रास सेक्शन पर आधारित परिणामों के साथ जोड़ा गया है।

ABSTRACT. The amplitude of analytic signal of real component of very low frequency electromagnetic (VLF-EM) and resistivity method were used to determine the location of fracture zone in part of hard rock area of Mirzapur district, Uttar Pradesh, India. The satellites Imagery was used to delineate the lineament besides prior information for appropriate locations using integrated geophysical surveys. The VLF-EM data was acquired along the six VLF traverses profiles. The results were obtained using Fraser and Karous-Hjelt filters to correlate with the Hilbert transform and amplitude of analytic signal of real component of VLF-EM data and the amplitude of the 2-D analytic signal of the real component in the form of an image of the profile. The real component of the Hilbert transform generates an approximate depth of fracture zone in part of hard rock area. It was correlated with results based on resistivity sounding and geoelectrical cross section.

Key words – Analytic signal, VLF-EM, Hilbert transform, VES, Mirzapur.

1. Introduction

The groundwater occurs in pore spaces between grains in alluvial and sedimentary rocks, in fractured zones of metamorphic rocks and openings in lavas formed at the time of their compaction. In India the importance of groundwater investigation has been realized due to the irregularity and failure of monsoon. It is essential to locate the aquifers and make correct estimates for regular supply of groundwater (Yadav and Singh, 1987). Groundwater occurs in limited areal extent in secondary porosity generally developed due to weathering, fracturing, jointing, faulting etc. within the hard rock areas. These structural changes (fractures etc.) are sparsely distributed in hard rock areas (Yadav and Singh, 2007).

In hard-rock areas, water-saturated fractures are randomly distributed. If the geoelectrical sounding is conducted randomly, then it may not coincide with the fractured zone and consequently fail to locate the presence of fractures at that point. For this reason, many geoelectrical sounding need to be conducted over the same area. However, before undertaking geoelectrical sounding, several approaches are adopted for conducting geophysical method to locate fracture zones in hard rock area (Yadav and Singh, 2008).The success of groundwater exploration projects had higher success rates when sites for drilling or detailed geophysical survey were guided by lineament mapping using satellite images (Teme and Oni, 1991; Gustafsson, 1993).

2. Study area

2.1. *Location and geographical of the study area*

The study area is the part of hard rock area of Mirzapur district, Uttar Pradesh. It is situated between latitude 24°58'23.41" to 25°00'55.42" North and longitude

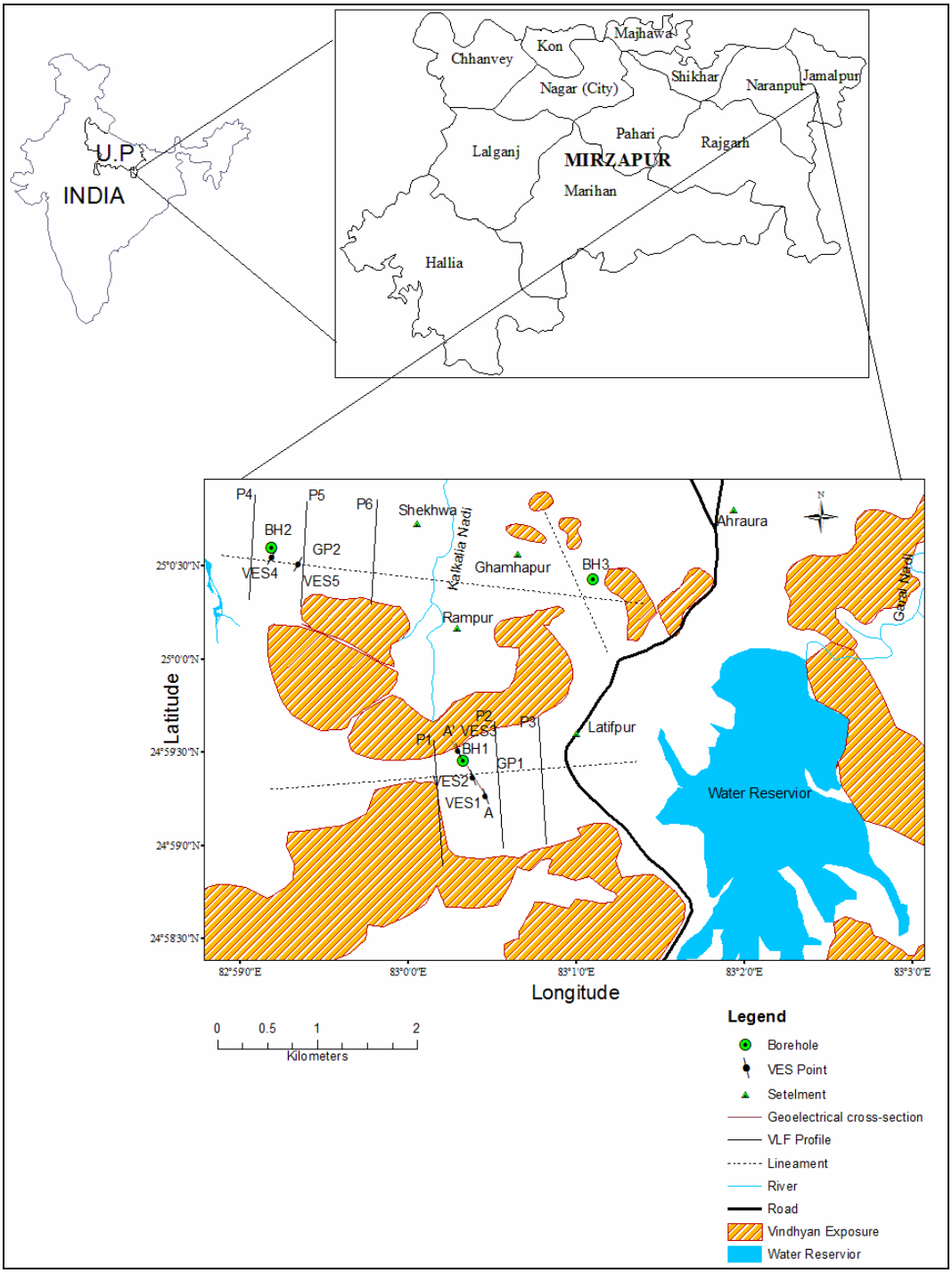

Fig. 1. Map of the study area

82°58'48.21" to 83°03'03.75" East and shown in Fig. 1 covering about 35 km^2. The area is taken from the Survey of India toposheet No.630/4 and 63P/1. The elevation ranges about 151 to 475 meter above mean sea level.

2.2. *Geology of the study area*

The area under investigation lies in the northern part of Vindhyan-terrain, situated in the south-eastern direction

of the river Ganges. Some part of the area falls on the northern slope of Vindhyan plateau which is entirely covered with a varying thickness of Pleistocene and recent alluvial deposits of the Gangetic river system. The outcrops of country rocks in the area are the Kaimur sandstones. In the southern region, more Vindhyan exposures are covered. (Yadav and Singh, 1987). The Vindhyan Supergroup is composed mostly of low dipping formations of sandstone, shale and carbonate, with a few conglomerate and volcaniclastic beds, separated by a major regional and several local unconformities (Bhattacharyya, 1996). The regional unconformity occurs at the base of the Kaimur Group and divides the sequence into two units: the Lower Vindhyans (Semri Group) and the Upper Vindhyans (Kaimur, Rewa and Bhander Groups). The outcrop pattern of the Supergroup resembles a simple saucer-shaped syncline. It is generally believed that the Vindhyan basin was a vast intra-cratonic basin formed in response to intraplate stresses (Bose *et al*., 2001). Groundwater in Kaimur Formation may occur in the weathered and fractured sand stone provided the zone is connected with recharging sources. The Kaimur Group of the Vindhyan Supergroup is of special significance because it consists dominantly of silica-clastic rocks lying unconformably over the carbonate-rich Semri Group - Lower Vindhyans. Therefore, the rocks from the Kaimur Group hold strong evidence regarding changing environment of deposition, climatic conditions and tectonics and weathering conditions, during Mesoproterozoic (Mishra and Sen, 2010).

3. Very low frequency electromagnetic (VLF-EM)

The very low frequency electromagnetic method (VLF-EM) is a passive method that uses radiation from about 42 worldwide ground-based military radio transmitters (used for navigation) operating in the VLF band (15-30 kHz). This gives primary electromagnetic (EM) field to determine the locations of saturated, sub-vertical conductive zones in which the primary electromagnetic (EM) wave induces current flow (Gnaneshwar *et al*., 2010). The induced currents produce secondary magnetic fields that can be detected at the surface through deviation of the normal radiated field. The radiated field from a remote VLF transmitter, propagating over a uniform or horizontally layered earth and measured on the earth's surface, consists of a vertical electric field component and a horizontal magnetic field component each perpendicular to the direction of propagation. The VLF unit is a sensitive receiver, covering the frequency band of the VLF - transmitting stations and capable of measuring the vertical components of the secondary field generated by lateral changes in conductivity in earth materials. McNeill and Labson (1991) showed that the induced current flowing in fracture zones usually produces a secondary magnetic field that is imaginary component with the primary magnetic field which would aid in the easy detection of fractures zone (Ndatuwong and Yadav, 2013). Fraser and Hjelt filtering and subsequent contouring of the observed responses are the most common practices to derive qualitative information about the subsurface (Fraser, 1969; Karrous and Hjelt, 1983).

Acquired VLF-EM data using WADI instrument was manufactured by ABEM. The procedure first consists of selecting a transmitter station which provides a field approximately parallel to the traverse direction, *i.e*., approximately perpendicular (or within ± 20°) to the expected strike of a conductor. The instrument measured the real (real component) and imaginary (out-of phase) components of the vertical to horizontal magnetic ratio (ABEM Instruction Manual). The VLF-EM data acquired along six VLF traverses at an operating frequency 18.2 and 19.7 KHz used for entire VLF survey. P1, P2 and P3 run north-south direction parallel to each other which are located at the central part of the study area. P4, P5 and P6 run approximately north-south direction parallel to each other which are located at the north western part of the study area. The distance between measurement points along the profile line was used 10 m and the distance between profile lines along profile direction was kept 50m while the profile length varied between 250 and 500 m.

4. Amplitude of the analytic signal

The amplitude of the analytic signal is being used extensively in the precise location of subsurface targets besides estimating the depth to the top based on certain characteristic points in the interpretation of gravity, magnetic, self-potential anomalies (Nabighian, 1972; Sundararajan *et al*., 2000 and Sundararajan and Srinivas, 2010). A similar approach for the location of fractures in hard rock area and subsequent interpretation can be applied to the real component IP(x) of VLF-EM data.

The analytic signal A(x) of function of real IP(x) component of VLF-EM data is expressed in Sundararajan *et al.* (2011) as :

$$A(x) = IP(x) + iHT\,[IP\,(x)] \quad (1)$$

The amplitude AA(x) of the Analytic signal can be calculated by the equation

$$AA(x) = \sqrt{IP(X)^2 + HT^2}\;[IP(x)] \quad (2)$$

where, HT[IP(x)] is the Hilbert transform of real component IP(x) of VLF-EM data that can be calculated as discussed by Sundararajan and Srinivas (2010).

(a)

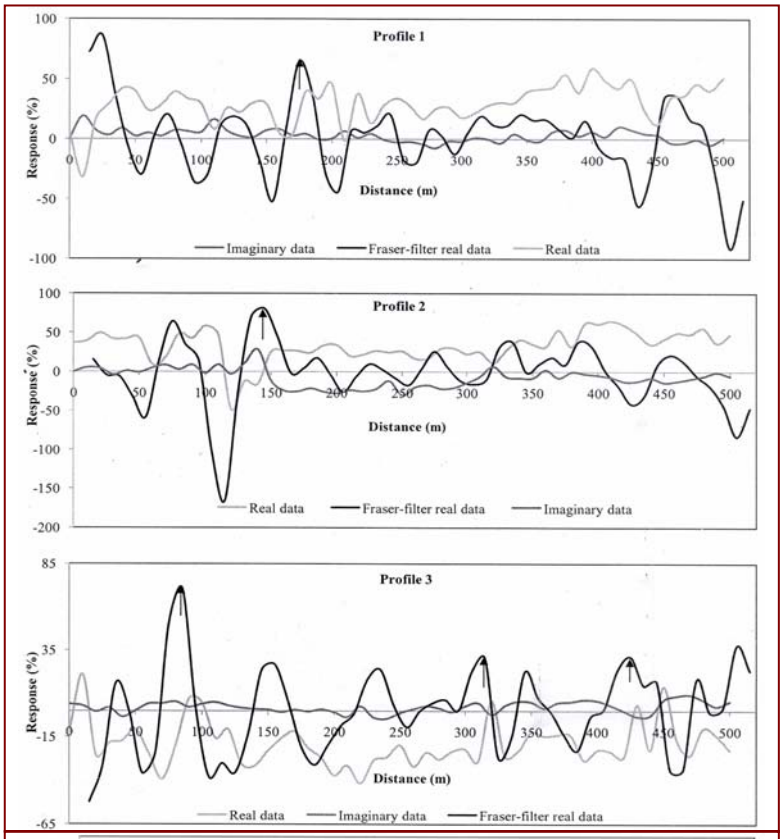

(b)

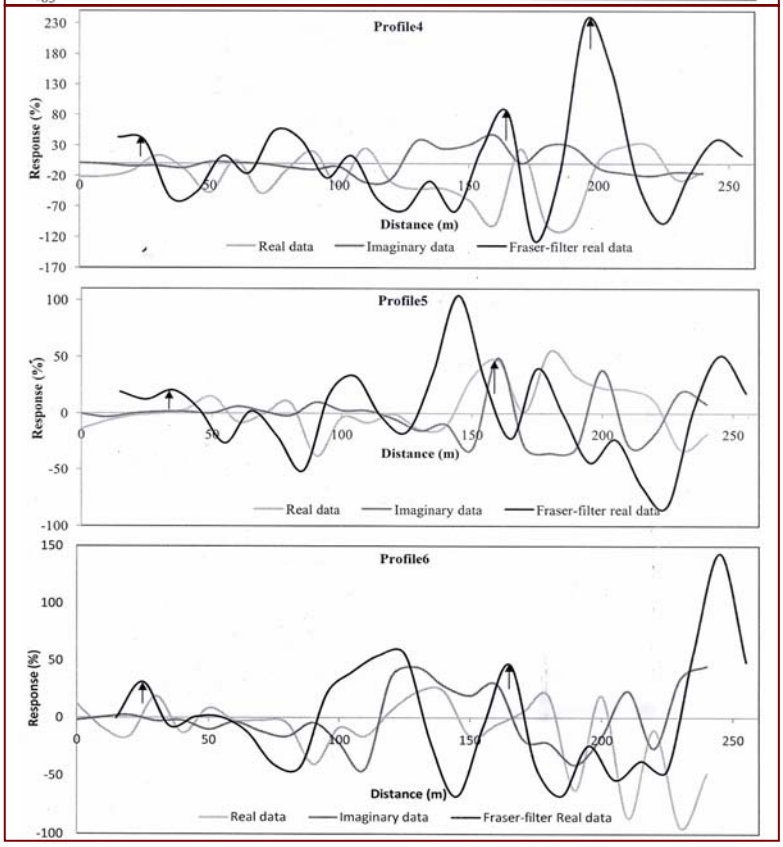

Figs. 2(a&b). Fraser-filtered real data curves for profiles P1, P2, P3, P4, P5 and P6

(a)

(b)

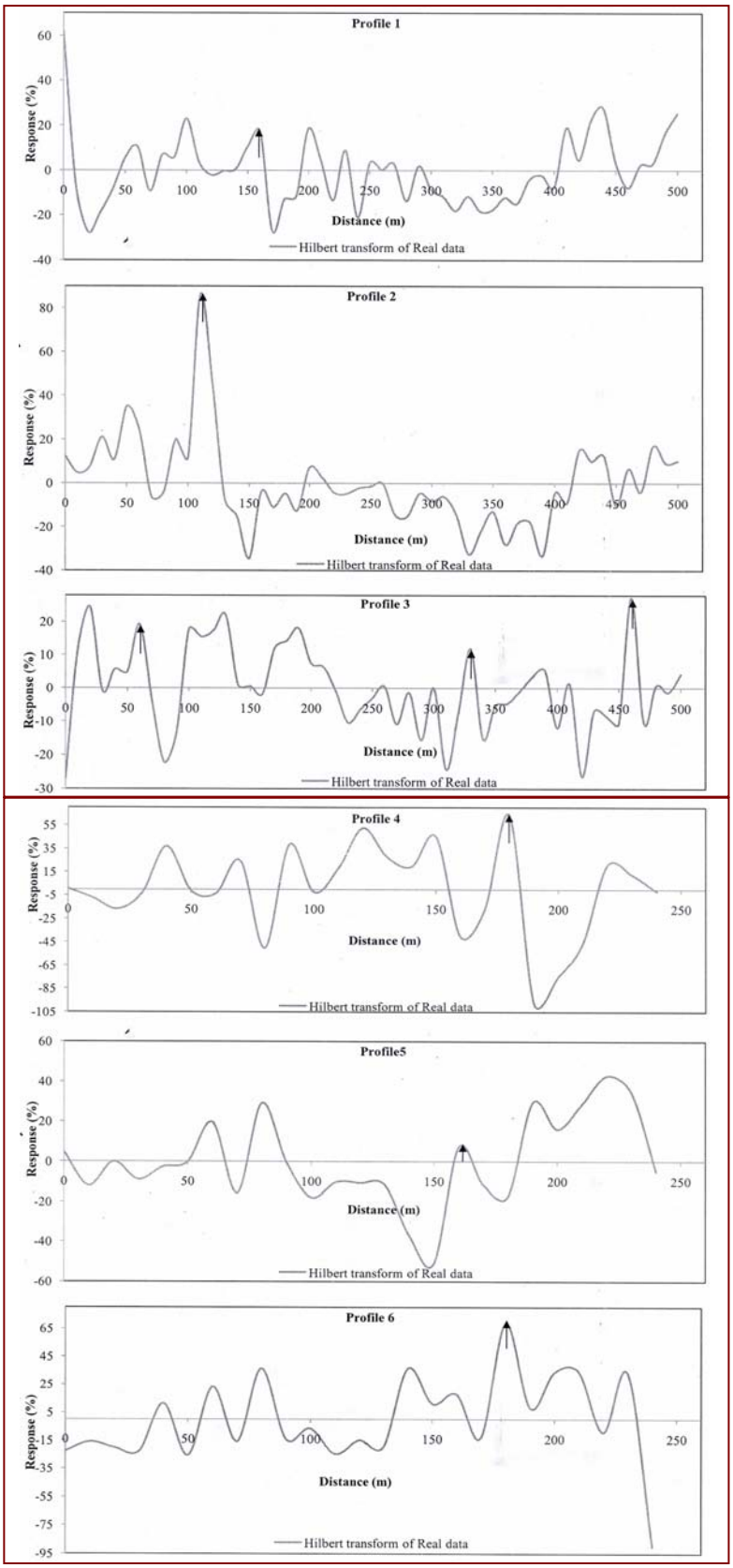

Figs. 3(a&b). Hilbert-transform of real data curves for profiles P1, P2, P3, P4, P5 and P6

(a)

(b)

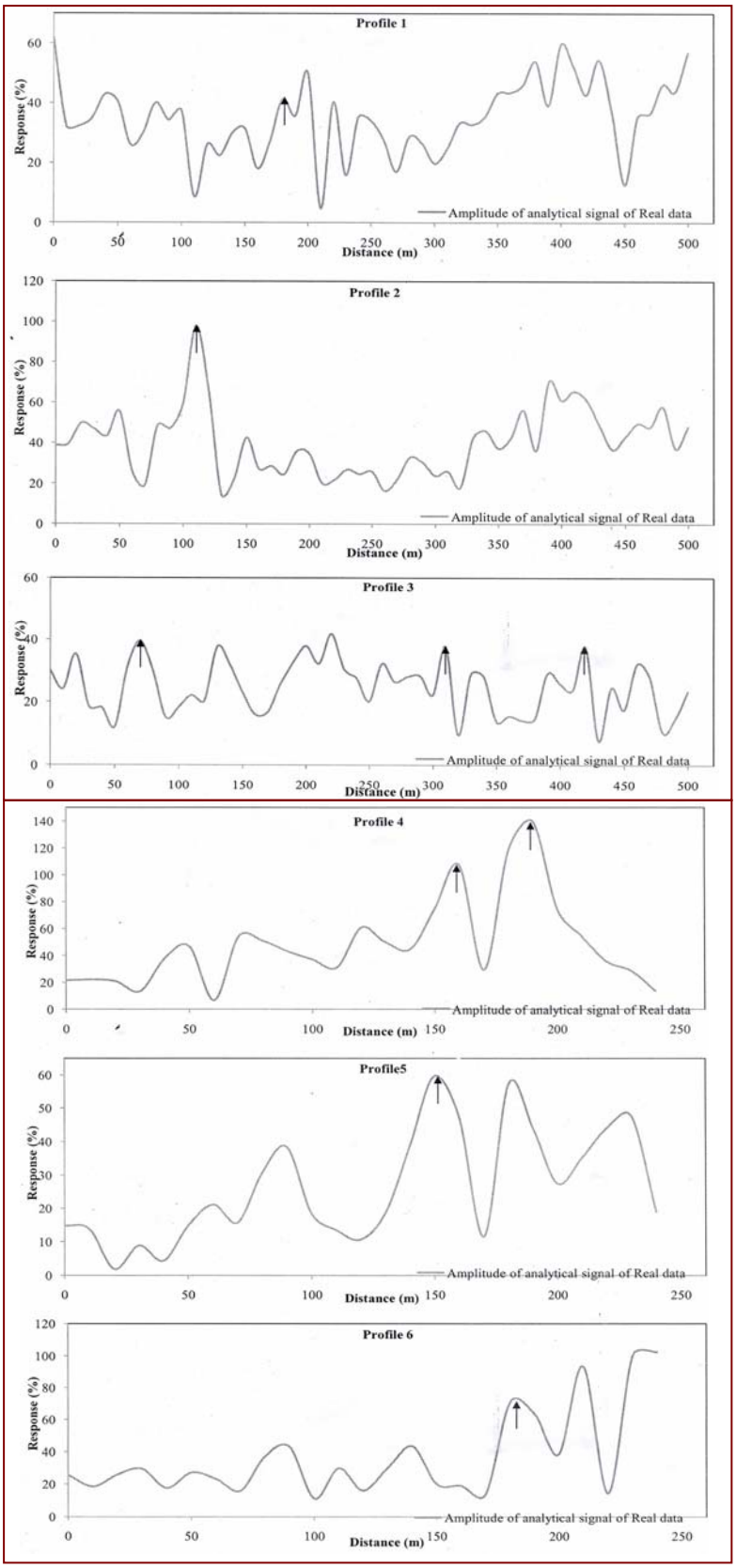

Figs. 4(a&b). Amplitude of analytic signal of real data curves for profiles P1, P2, P3, P4, P5 and P6

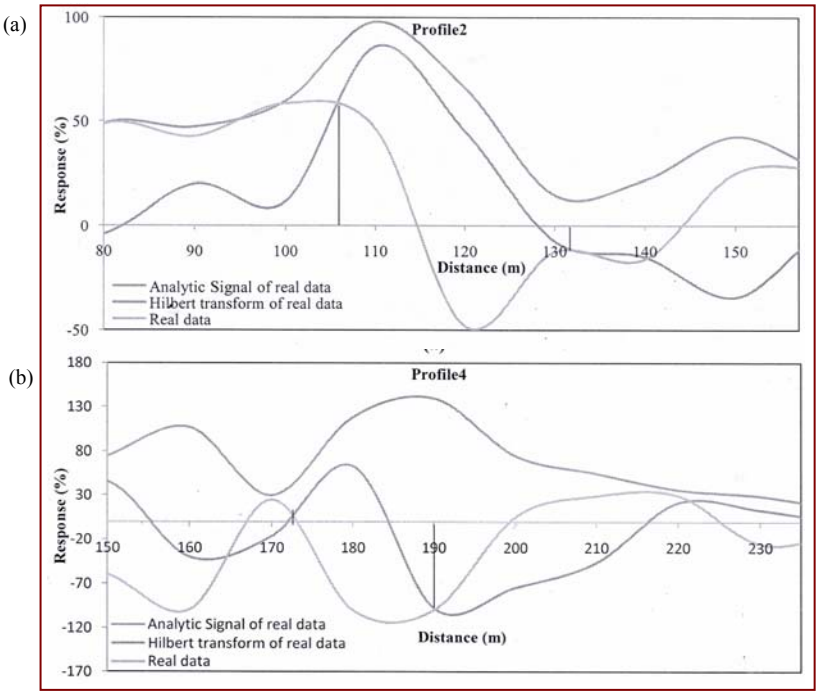

Figs. 5(a&b). (a) The real data of traverse P2, the Hilbert transform and the amplitude of analytic signal of real data (b) The real data of traverse P4, the Hilbert transform and the amplitude analytic signal of real data

5. Results and discussion

5.1. *Fraser and Karous-Hjelt filtering results*

The measured real and imaginary VLF-EM data were processed using Fraser (1969) filtering technique which completely removes dc bias, greatly attenuates long wavelength signals and completely removes Nyquist frequency related noise besides phase shifts all frequencies by 90°. It has the band pass centered at a wavelength of five times the station spacing (Sundararajan *et al*., 2011). The Fraser filter (Fraser 1969) converts crossover points into peak responses by 90° phase shifting. This process reduces the random noise between consecutive stations resulting from very low frequency component of sharp irregular responses (Al-Tarazi *et al*., 2008). The Fraser filter real part will always show a positive peak above a conductor, while the imaginary part can show a positive as well as a negative peak depending on the overburden layer. The imaginary part is of some value when making decision about the quality of the conductor (Ariyo *et al*., 2009).

The real and imaginary raw data were plotted against station positions with the Fraser-filtered real data on the secondary axis of the same graph. The graph was analysed for crossovers and peaks. A stacked profile of the Fraser-filtered real data of the VLF-EM profiles are presented in Figs. 2(a&b) with the crossover points (marked with thick arrows). A qualitative interpretation is based on the crossover point between the real and imaginary data which appears as positive peaks in the Fraser-filtered real curve; these regions constitute anomalous zones which can be attributed to the presence of vertical conductor or lateral contacts of different resistivities beneath the surface (Srigutomo *et al*., 2005).

5.2. *Hilbert-transform and amplitude of analytic signal of real component*

Both real and imaginary components contain valuable diagnostic information about subsurface targets. However, only a few schemes exist for extracting the required information and thereby relating the observed anomalies to the causative source. Although Fraser and Karous-Hjelt filtering techniques provide first hand information regarding the number, size, depth and relative disposition of the discrete conductors, the disadvantage with these filters is loss of 20 to 30% of data on either side of the profile, which sometimes complicates the interpretation of the data (Sundararajan *et al*., 2011). Further, the interpretation of VLF-EM data is not as

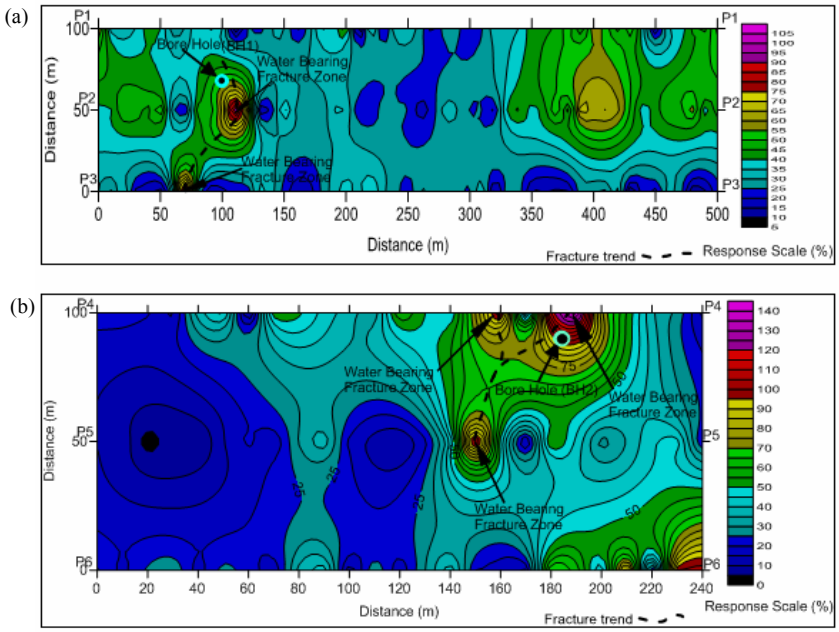

Figs. 6 (a&b). (a) Amplitude of the 2-D analytic signal of the real component of the profiles P1 to P3 (b) Amplitude of the 2-D analytic signal of the real component of the profiles P3 to P6

simple as other geophysical anomalies because the relatively high transmitter frequency gives rise to secondary fields from many geological features which are electrically conducting (Phillips and Richards 1975). Also, the three dimensionality of the geological structure complicates the 2D inversion of VLF-EM data. The quantitative interpretation of single frequency VLF-EM data was examined by several authors (Coney, 1977; Beamish, 2000).

Alternatively, the use of the Hilbert transform for the interpretation of VLF-EM data in analogy with the magnetic anomalies is explored in this paper. The application of the Hilbert transform to the real component shifts the phase of all spatial frequencies by 90°, that is, it turns crossovers into peaks or troughs (marked with thick arrows). These peaks can be interpreted in terms of conductors. Thus, the Hilbert transform can be deciphered somewhat similarly to the Fraser filter, or, the Hilbert transform and the Fraser filter do a similar job to some extent (Sundararajan *et al*., 2011). Here, the Hilbert transform of the real component of all the six traverses profiles namely P1 to P6 are computed traverse wise and shown in Figs. 3(a&b) and analytic signal are useful in delineating the fractures zone in part of hard rock area.

The spatial location of conductors can be realized precisely from the amplitude of the analytical signal (Sundararajan, 1983; Sundararajan *et al*., 1998). Equation (2) was used to compute the amplitude of the analytic signal for each traverses namely P1 to P6 shown in Figs. 4(a&b).

The Hilbert transform of the traverses P2 and P4 are computed for possible depth estimation in analogy with the interpretation of gravity/magnetic/self potential data (Sundararajan, 1983; Sundararajan and Srinivas, 1996). The computed Hilbert transform and the amplitude of the analytic signal of traverses P2 and P4 are shown in Figs. 5(a&b).

Based on certain characteristic points of the amplitude of the analytic signal and the abscissa of the point of intersection of the real component and its Hilbert transform of traverses P2 and P4 shown in Figs. 5(a&b) (Sundararajan *et al*., 2011). The intersection points of real component of very low frequency electromagnetic (VLF-EM) IP(x) and its Hilbert transform HT[IP(*x*)] with certain characteristic points of the amplitude of the analytical signal AA(*x*) are used to determine the depth of the fracture zone in hard rock area from the top of surface. The depth of fracture zone from top of surface can be estimated as (Sundararajan and Srinivas, 2010).

$$h = (x_1 + x_2)/2 \qquad (3)$$

where, x_1 and x_2 are intersection points of the real component and its Hilbert transform of very low

TABLE 1

Geoelectrical and lithological parameters of the vertical electrical sounding (VES)

VES No.	No of layers	Resistivity (Ω-m)	Thickness (m)	Depth (m)	Lithology
01	5	90	2.77	0.0	Surface soil
		8568	9.82	2.77	Compact sandstone
		69.01	35.09	12.60	Fractured sandstone
		367.07	166.07	47.69	Semi-fractured sandstone
		18,9880	-	213.77	Compact sandstone
02	5	60	3.33	0.0	Surface soil
		39326	6.62	3.33	Compact sandstone
		168.73	10.30	9.95	Fractured sandstone
		20286	260.51	20.26	Compact sandstone
		17,4420	-	280.77	Compact sandstone
03	5	250	2.62	0.0	Surface soil
		22674	7.41	2.62	Compact sandstone
		49.67	111.03	10.04	Fractured sandstone
		1846.40	28.83	121.08	Semi-compact sandstone
		20,5110	-	149.91	Compact sandstone
04	6	23	0.15	0.0	Surface soil
		1.38	0.10	0.15	Clay
		2981.90	4.14	0.25	Semi-compact sandstone
		0.71	66.08	4.39	Clay
		33.99	82.73	70.48	Fractured sandstone
		4295.50	-	153.22	Semi-compact sandstone
05	6	80	1.22	0.0	Surface soil
		0.52	0.29	1.22	Clay
		7615.40	1.08	1.52	Semi-compact sandstone
		1.80	43.13	2.61	Clay
		706.95	29.42	45.74	Semi-fractured sandstone
		20327	-	75.16	Compact sandstone

frequency electromagnetic (VLF-EM) and *h* is the depth of fracture zone from top of surface. Thus, the approximate depths of the fracture zone in part of hard rock area from top of surface are found to be 15m (traverse P2) and 7m (traverse P4) respectively.

6. 2-D image of the amplitude of the analytic signal of real component

The 2-D image of the amplitude of the analytic signal is shown in the Figs. 6(a&b). Two water bearing fracture zones and also trend of the fracture are identified by the 2-D image of the amplitude of the analytic signal of real component of VLF-EM data shown in Fig. 6(a). Fig. 6(b) shows, three water bearing fracture zones and also fracture trend are identified by the 2-D image of the amplitude of the analytic signal of real component. These images very clearly bring out the water bearing fracture zones and fracture trend in the part of hard rock area. The boreholes (BH1 and BH2) existed closely to the water saturated fracture zones and along fracture trend shown in Figs. 6 (a&b) which can be seen in the field and also shown in study map.

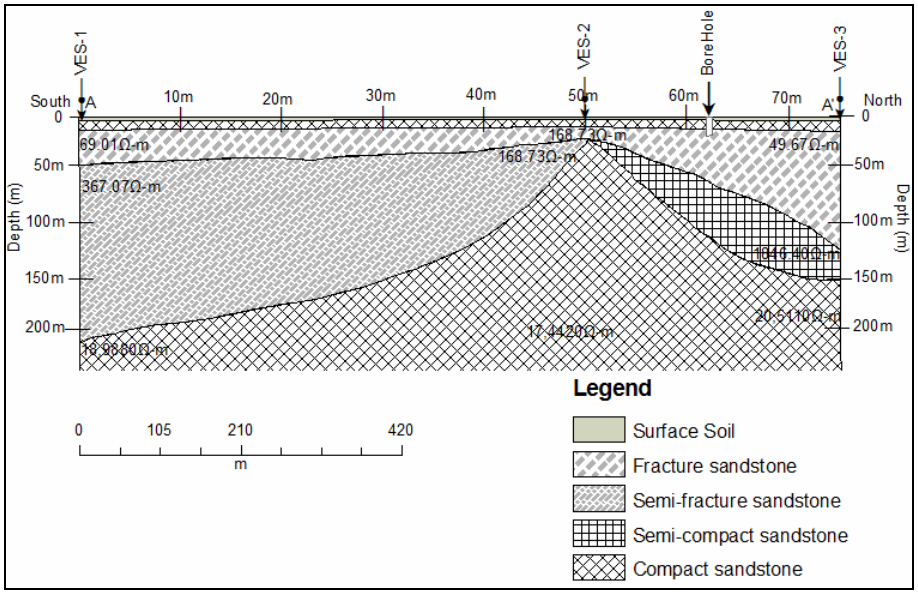

Fig. 7. Geoelectrical cross-section along profile AA'

7. Vertical electrical sounding (VES) andgeoelectrical cross-section AA'

Five Vertical electrical sounding (VES) were conducted around the identified anomalous zones using Schlumberger configuration. The apparent resistivity values obtained from the field were plotted against half current electrode spacing on log-log graph paper. The layer parameters were initially obtained using initial curve matching technique (Keller and Frischknecht, 1966; Bhattacharya and Patra, 1968; Koefoed, 1979) and auxiliary point charts (Ebert, 1943). A Terrameter SAS 1000 (manufacturer; ABEM, Sweden) was used to conduct electrical resistivity survey from study area. These parameters were used as initial model for computer assisted interpretation program AIMRESI (Automatic Iterative Method of Resistivity Sounding Interpretation) developed by Yadav (1995). The geoelectrical and lithologic parameters are presented in the Table 1.

VES-1 was carried out approximately at 140m of VLF-EM profile P2. VES-2 was conducted just approximately 50 m southeast of VES-1. VES-3 was also conducted along southeast direction and approximately 25 m of VES-2. All three vertical electrical sounding (VES-1, VES-2 and VES-3) are placed approximately linearly along southeast direction and indicates the geoelectrical cross-section AA' shown in Fig. 1. All three vertical electrical soundings (VES) shows a five-layer model. The upper layer having a resistivity approximately 60 to 250 Ω-m and indicates surface soil with the thickness approximately 2.62 to 3.33 m. The resistivity of the second layer abruptly increases approximately 8568 to 39326 Ω-m, which indicates compact sandstone with a thickness approximately 6.62 to 9.82 m. The third layer represents a highly-fractured layer having thickness of about 10.30 to 111.03 m and low resistivity value may be due to presence of highly-fractured saturated sandstone which may have been a good zone for groundwater exploration. Again, resistivity value increases and fourth layer represents semi-fractured sandstone. The last layer at depth of about 149.91 to 280.77 m represents the resistive substratum with a high resistivity value of about 17, 4420 to 20,5110 Ω-m.

The cross section AA' between VES-1 to VES-3 is based on results of the three vertical electrical soundings is shown in Fig. 7 and also shows hard rock area. This profile lies to the west of the Ahraura reservoir. The thin upper layer is present with varying thickness all along profile and average thickness about 2.90 m. The resistivity of this layer is not uniform due to variation in moisture content and soil type of layer. Below this layer thin compact sandstone and thickness is approximately uniform. The fractured sandstone occurs all along profile. The thickness of this layer is approximatly uniform from VES-1 to VES-2 and gradually increases toward sounding VES-3. The lithological information from existing borehole correlate to the portion of the cross section in between the sounding VES-2 to VES-3 and which shows good similarity between both results. In the southern

portion of the cross section, thick semi fracture sandstone is present from sounding VES-1 to VES-2 and thickness of this layer gradually descreases toward VES-2. In northern portion of the cross section, semi compact sandstone is present from sounding VES-2 to VES-3. The thick fracture sandstone indicates good potential of ground water in hard rock area and is present in between sounding VES-2 and VES-3 and can be exploited for drinking purposes.

VES-4 was carried out approximately at 180 m of VLF-EM profile P4. VES-5 was conducted just approximately 60 m east of VES-4. Both vertical electrical soundings (VES-4 and VES-5) shows a six-layer model. The first layer has a resistivity approximately 23 to 80 Ω-m with a thickness approximately 0.15 to 1.22 m. The resistivity of the second layer approximately 0.52 to 1.38 Ω-m with a thickness approximately 0.10 to 0.29 m. Both layers extended up to a depth of about 0.25 to 1.52 m and indicate the presence of surface soil which is made up of clay. The resistivity of the third layer abruptly increases approximately 2981.90 to 7615.40 Ω-m, which indicates semi-compact sandstone. The fourth layer represents thick layer of clay with the resistivity approximately 0.71 to 1.80 Ω-m and thickness approximately 43.13 to 66.08 m. This thick layer occurs below the semi-compact sandstone (hard rock). This condition may be possible when fracture zone occurs. So the highly-fractured zone occurs below the depth approximately 2.61 to 4.39 m. The fifth layer represents semi-fractured sandstone with the resistivity approximately 33.99 to 706.95 Ω-m and thickness approximately 29.42 to 82.73 m. The last layer is compact sandstone with a resistivity of the order 4295.50 to 20327 Ω-m at the depth approximately 75.16 to 153.22 m. Geoelectrical cross section was not created close to the EM-profile P4 because for geoelectrical cross section at least three vertical electrical sounding are required but here only two vertical electrical soundings (VES) are present as shown in Fig. 1.

8. Conclusions

The integrated geophysical method (very low frequency electromagnetic (VLF-EM) and resistivity vertical geoelectrical sounding (VES) using Schlumberger configuration) delineated fracture zones in part hard rock area in Mirzapur district, Uttar Pradesh for groundwater exploration. The amplitude of the analytic signal indicated the exact location of subsurface feature. Also, the Hilbert transform was useful for the evaluation of the depth of the top of the fracture zones in part of hard rock area. The depth of fracture zone evaluated by the Hilbert transform approximately correlated with the result of vertical electrical sounding (VES).

Acknowledgement

The authors wish to thank the Head of Department of Geophysics, B. H. U., Varanasi, India for providing the necessary facilities required for geophysical survey and also thankful to Mr. Ram Mohan for support during the survey.

References

ABEM Instruction Manual ABEM WADI VLF INSTRUMENT http://www.abem.se.

Al-Tarazi, E., Abu Rajab, J., Al-Naqa, A. and El-Waheidi, M., 2008, "Detecting leachate plumes and groundwater pollution at Ruseifa municipal landfill utilizing VLF-EM method", *J. Appl. Geophys*., **65**,121-131.

Ariyo, S. O., Adeyemi, G. O. and Oyebamiji, A. O., 2009, "Electromagnetic VLF survey for groundwater development in contact terrain; a case study of Ishara-reno, South Western Nigeria", *J. Appl. Sci. Res*., **5**, 9, 1239-1246.

Beamish, D., 2000, "Quantitative 2D VLF data interpretation", *J. Appl. Geophys.*, **45**, 33-47.

Bhattacharyya, A., 1996, "Recent advances in Vindhyan", *Geology Geol. Soc. India Memoir*, **36**, 331-337.

Bhattacharya, P. K. and Patra, H. P., 1968, "Direct current geoelectric sounding", Elsevier, Amstardam, p135.

Bose, P. K., Sarkar, S., Chakrabarty, S. and Banerjee S., 2001, "Overview of Meso- to Neoproterozoic evolution of the Vindhyan basin", *Central India J. Sediment. Geol*., **142**, 395-419.

Coney, D. P., 1977, "Model studies of the VLF-EM method of geophysical prospecting", *Geoexploration*, **15**, 19-35

Ebert, A., 1943, "Grundlagen zur Auswerkung geoelektriscer Tiefenmr-ssulgon, Garlands Beitrage Zur Geopysik", *BZ*, **10**, 1, 1-17.

Fraser, D. C., 1969, "Contouring of VLF-EM data", *Geophys*., **34**, 958-967.

Gnaneshwar, P., Shivaji, A., Srinivas, Y., Jettaiah, P. and Sundararajan, N., 2010, "Very-low-frequency electromagnetic (VLF-EM) measurements in the Schrimacheroasen area, East Antarctica", *Polar Sci*., **5**, 1, 11-19.

Gustafsson, P., 1993, "Satellite data and GIS as a tool in groundwater exploration in semi-arid area Publication A 74", Chalmers University of Technology, Gothenburg.

Karous, M. and Hjelt, S. E., 1983, "Linear filtering of VLF dip angle measurements", *Geophys. Prospect*., **31**, 782-794.

Keller, G. V. and Frischknecht, F. C., 1966, "Electrical methods in geophysical prospecting", Pergamon press, New York, p519.

Koefoed, O., 1979, "Geosounding principles, 1: resistivity sounding measurements", 14A Elsevier, Amsterdam.

McNeill, J. D. and Labson, V. F., 1991 "Geological mapping using VLF radio fields", In: Nabighian M (ed) Electromagnetic methods in applied geophysics", Vol. 2, part B, Society of Exploration Geophysics, Tulsa, 521-640.

Mishra, M. and Sen, M., 2010, "Geochemical signatures of Mesoproterozoic silica-clastic rocks of the kaimur group of the Vindhyan Supergroup, Central India", *Chin. J. Geochem*., **21**, 21-32.

Nabighian, M. N., 1972 , "The analytical signal of 2D magnetic bodies with polygonal cross section, its properties and use for automated anomaly interpretation", *Geophysics*, **37**, 507-512.

Ndatuwong, L.G. and Yadav, G. S., 2013, "Identifications of fractured zones in part of hard rock area of Sonebhadra District, U.P., India using integrated surface geophysical method for groundwater exploration", *J. Arab. Geosci*.,doi:10.1007/s12517-013-0880-y.

Phillips, W. J. and Richards, W. E., 1975, "A study of the effectiveness of the VLF method for the location of narrow mineralized zones", *Geoexploration*, **13**, 215-226.

Srigutomo, W., Harja, A., Sutarno, D. and Kagiyama, T., 2005, "VLF data analysis through transformation into resistivity value: application to synthetic and field data", *Indones. J. Phys*., **16**, 4, 127-136.

Sundararajan, N., 1983, "Interpretation techniques in geophysical exploration using Hilbert transform PhD Thesis", Osmanai University, Hyderabad.

Sundararajan, N. and Srinivas, Y., 1996, "A modified Hilbert transform and its application to self potential interpretation", *J. Appl. Geophys*., **36**, 137-143.

Sundararajan, N. and Srinivas, Y., 2010, "Fourier Hilbert versus Hartley Hilbert transforms with some geophysical applications", *J. Appl. Geophys.*, **71**, 157-161.

Sundararajan, N., Srinivas, Y. and Rao, T. L., 2000, "Sundararajan transform - A tool to interpret potential field anomalies", *Explor. Geophys*., **31**, 621-628.

Sundararajan, N., Srinivasa Rao, P. and Sunitha, V., 1998, "An analytical method to interpret self-potential anomalies caused by 2D inclined sheets", *Geophysics*, **63**, 1151-1155.

Sundararajan, N., Babu, V. R. and Chaturvedi, A. K., 2011, "Detection of basement fractures favourable to uranium mineralization from VLF-EM signals", *J. Geophys. Eng*., **8**, 330-340.

Teme, S. C. and Oni, S. F., 1991, "Detection of groundwater flow in fracture media through remote sensing technique - Some Nigerian cases", *J. Afr. Earth. Sci*., **12**, 3, 461-466.

Yadav, G. S., 1995, "A FORTRAN computer program for the automatic interactive method of resistivity sounding interpretation", *Acta Geodaetica et Geophysica Hungarica*, **30**, 2-4, 363-377. View Record in Scopus | Cited By in Scopus (3).

Yadav, G. S. and Singh, C. L., 1987 "Groundwater Investigations using Schlumberger sounding in the Vindhyan Fringe Belt of Ahraura Region, Mirzapur (U.P.)", *J. Assoc. Expl. Geophys*., **8**, 4, 237-245.

Yadav, G. S. and Singh, S. K., 2007, "Integrated resistivity survey for the delineation of fractures for ground water exploration in hard rock areas", *J. Appl. Geophys*., **62**, 3, 301-312.

Yadav, G. S. and Singh, S. K., 2008, "Gradient profiling for the investigation of ground water saturated fractures in hard rocks of Uttar Pradesh", *India Hydrogeol. J*., **16**, 363-372.